Caspian Journal of Environmental Sciences
Online ISSN: 1735-3866
Print ISSN: 1735-3033

Analyzing the relationship between geographical elements and precipitation patterns in the southern shores of the *Caspian Sea*

Kamal Omidvar[1], Mahdi Narangifard[1], Mehran Fatemi[*2]

1. Department of Geography, Yazd University, Yazd, Iran
2. Department of Climatology, Meybod University, Meybod, Iran

** Corresponding author's E-mail: yazdfatemi@meybod.ac.ir*

ABSTRACT

The present study focuses on the distribution of precipitation in different spatial and temporal patterns based on monthly, seasonal and annual time scales using TRMM data derived from 92 different cells in the south of the Caspian Sea. In addition, to account for the impact of the geographical conditions such as elevation, latitude and longitude on rain values, the Pearson correlation method was used. In terms of the average monthly precipitation in the south of the sea, the results showed that the highest average belonged to November (87 mm), followed by December (74 mm), and finally March and October (67 mm and 66 mm), respectively. The highest negative correlation (0.862) between rain and longitude was observed in autumn at a significant level of 0.01. In addition, the highest negative correlation (0.87) between rain and longitude was found in November at a significant level of 0.01. The maximum annual rain was 892-1305 mm measured in Guilan Province. Precipitation showed a tendency to decline toward the east of Golestan Province, so that the minimum annual precipitation (321-393 mm) was recorded in its western and northeastern parts. The precipitation was positively correlated with elevation and there was a strong inverse relationship between rain and longitude.

Keywords: Caspian Sea, Rain, Correlation, TRMM.
Article type: Research Article.

INTRODUCTION

Precipitation, as a key component of the global water cycle, serves as a major parameter in ecology, hydrology and meteorology. Precipitation data with accurate, high spatial resolution are crucial for broadening our understanding of basin-scale hydrology (Jia *et al.* 2011). It is a critical meteorological parameter that needs to be measured accurately. Numerous applications of precipitation data can be studied with an in-depth knowledge of its actual distribution (Almazroui, 2011). It plays a vital role in energy exchange and material circulation in the surface system of the earth. Therefore, it is of paramount importance to understand the spatial and temporal variations of precipitation. Traditional precipitation data is usually derived from point measurements, which rely heavily on field observations (Jia *et al*. 2011). Moreover, precipitation is an important climatic aspect that has both spatial and temporal variations. Understanding the behavior of precipitation and analyzing its spatial and temporal variations can contribute to comprehensive and detailed planning for water resource management and agriculture (Sotodeh & Alijani 2015). Remote sensing can provide spatial precipitation patterns (Immerzeel *et al.* 2009). The remote sensing of precipitation, by the satellite-borne remote sensor is of utmost importance. At first, precipitation exerts a great impact on the propagation of millimeter radio waves between satellites and the earth. Secondly, the global observation of precipitation by satellite-borne remote sensors is amenable to the monitoring of weather and climate variations. Meteorological satellites can obtain cloud images using visible and IR sensors. However, these sensors do not shed light on the actual occurrence and distribution of precipitation under the clouds (Okamoto *et al.* 1979). The tropical precipitation measuring mission (TRMM) was launched in November 1997, while the onboard precipitation radar was put in the observation mode in December 1997 (Gabella *et al.* 2011). After a decade, TRMM satellite has provided researchers with huge precipitation data that could be used for the validation of atmospheric and climate models. Given operational difficulties over the oceans, it is not

Caspian Journal of Environmental Sciences, Vol. 20 No. 1 pp. 89-99 Received: June 29, 2021 Revised: Sep. 05, 2021 Accepted: Oct. 16, 2021
DOI: 10.22124/CJES.2022.5395

Publisher: University of Guilan, Iran

possible to measure precipitation with rain gauges, thus remotely sensed information about precipitation provides the only source of reliable and continuous data (Shrivastava *et al*., 2014). TRMM 3B42 generally offers a smoother precipitation field than gauge data, which is due to the temperature structure of clouds. In the areas of elevated gauge density, TRMM 3B42 is of comparatively coarser spatial resolution. An approximately real-time estimate of precipitation based on satellite measurements is available with a nine-hour time lag at three-hour intervals. Additional estimates calibrated with ground measurements are subsequently produced 10-15 days after the end of the month (Duncan & Biggs 2012). Satellite-based precipitation remote sensing has been a fertile research field for over three decades (Liu & Fu 2010). Studies based on TRMM satellite data have been undertaken in some regions such as the Middle East (Ud din et al. 2008; Javanmard et al. 2010; Almazroui 2011; Ahmadi & Narangifard 2012; Moazami et al. 2013; Shirvani & Fakhari Zade Shirazi 2014; Omidvar & Narangifard 2015; Javanmard & Jamli 2015; Mozafari & Narangifard 2016; Siabi *et al*. 2017; 25. Akbari Yangehghaleh *et al.* 2018), India (Mishra *et al.* 2012; Shrivastava *et al.* 2014), Nepal (Duncan & Biggs 2012), Bangladesh (Moffitt *et al.* 2011), China (Chen *et al.* 2011; Jia *et al.* 2011; Li *et al.* 2012; Du *et al.* 2013), Iberian Peninsula (Immerzeel *et al.* 2009), Peninsular Malaysia (Varikoden *et al.* 2010), Palestine West Bank (Khalaf & Donoghue 2012), and the United States (Puri *et al.* 2011). This study aimed to investigate spatial and temporal patterns of rain analysis as well as the impact of geographical conditions on precipitation in the southern parts of the Caspian Sea using TRMM satellite data.

MATERIALS AND METHODS

The Caspian Sea, with a surface area of 400000 km^2, is the largest inland water body in the world (Roohi *et al*. 2008). The study area is located in the south of the Caspian Sea, north of Iran (Fig. 1).

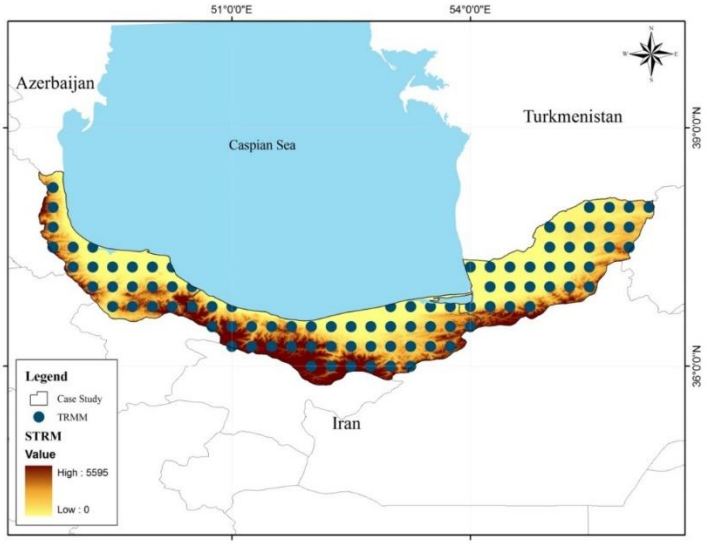

Fig. 1. Study area, elevation and location of the TRMM.

The TRMM is a joint US–Japan satellite mission undertaken for monitoring tropical and subtropical precipitation, and estimating associated latent heats. The TRMM was successfully launched on 27th November, 1997 from the Tanegashima Space Center in Japan (Kummerow *et al*. 1998). The TRMM includes a number of precipitation-related instruments, such as precipitation radar, a visible and infrared sensor (VIRS), and a SSM/Ilike TRMM microwave imager (TMI) (Kummerow *et al.* 2000). TRMM dataset 3B43 V6 between 50° south and 50° north was used to measure precipitation. TRMM data has become a reference standard compared to data derived from all other satellites. In this study, TRMM 3B43 dataset was used (http://disc2.nascom.nasa.gov). These gridded estimates have a calendar-month temporal resolution and a spatial resolution of 0.25° × 0.25°. Given that this study deals with the downscaling algorithm of precipitation, monthly, seasonal and annual precipitations from 1998 to 2013 were calculated by accumulating the monthly TRMM 3B43 data for each year. In this study, precipitation was estimated in 92 different locations in the south of the Caspian Sea on a monthly, seasonal and annual basis using TRMM data derived from 92 different cells in the southern parts of the Caspian Sea.

To assess the effects of elevation, latitude and longitude on the rain derived from TRMM 3B43 for the study period (1998-2013), Pearson correlation was used. Also, spatial distribution maps were generated using Surfer 10 software.

The Pearson correlation, which is commonly used for numerical variables, assigns a value in the range of -1 and 1, where 0 denotes lack of correlation, 1 indicates a complete positive correlation, and -1 denotes a complete negative correlation. A correlation value of 0.7 between two variables indicates that there is a significant and positive relationship between the two variables. The Pearson correlation between two data points X and Y is calculated as follows:

$$Correlation\ (X,Y) = \frac{s_{xy}}{s_x \times s_y}$$

where s_{xy} is the covariance of X and Y, which is computed as:

$$s_{xy} = \frac{1}{n-1}\sum_{i=1}^{n}(x_i - \bar{x})(y_i - \bar{y})$$

and s_x and s_y are standard deviation of X and Y, respectively.

RESULTS AND DISCUSSION

In this study, the spatial distribution of rain was calculated on a monthly, seasonal and annual basis in 92 different locations (cells) using TRMM data. Also, to account for the impacts of geographical conditions such as elevation, latitude and longitude on precipitation, the Pearson correlation was utilized.

Elevation, longitude and latitude –precipitation relationship

In all time scales (monthly, seasonal and annual scales), the Pearson correlation between longitude and rain was significant at a confidence level of 99%.

According to Table 1, longitude was highly correlated with precipitation in autumn, especially in November.

The results exhibited that precipitation dropped by longitude (Table 1). The strongest correlation between precipitation and longitude (R = 0.87) with a coefficient of determination of $R^2 = 0.756$ was observed in November while the weakest (R = -0.526) with $R^2 = 0.276$ in April. Thus, precipitation and longitude were not inversely correlated.

Table 1. Pearson correlation between rain and elevation, longitude and latitude.

Par	Longitude	Latitude	Elevation	Spring	Summer	Fall	Winter
Lon	1	-	-	-.633**	-.719**	-.862**	-.813**
Lat	-	1	-	.102	-.032	-.100	-.096
Elev	-	-	1	.249	-.047	.035	.109
Par	**Annual**	**Jan**	**Feb**	**Mar**	**Apr.**	**May**	**June**
Lon	-.829**	-.789**	-.732**	-.659**	-.526**	-.657**	-.789**
Lat	-.061	-.103	.003	-.051	.137	.263*	-.149
Elev	.084	.094	.080	.201	.298	.203	.039
Par	**July**	**Aug**	**Sep**	**Oct**	**Nov**	**Dec**	
Lon	-.625**	-.708**	-.814**	-.869**	-.870**	-.849**	
Lat	-.085	.057	-.039	-.130	-.116	-.134	
Elev	-.035	-.094	-.065	.066	.081	.129	

**Correlation is significant at 0.01 level
*Correlation is significant at 0.05 level

Given the average monthly precipitation in the south of the Caspian Sea, the highest precipitation (87 mm) was observed in November followed by December (74 mm), March (67 mm) and October (66 mm; Fig. 2). The seasonal distribution of precipitation is also shown in Fig. 3 exhibiting that autumn had the highest precipitation (32%), followed by winter (31%), spring (25%), and summer (12%).

Spatial and temporal pattern of precipitation

In January, the highest precipitation (80-129 mm) was recorded in Guilan Province, while the lowest in the western parts of Golestan Province (34-44 mm; Fig. 4). The precipitation was analyzed based on the Pearson correlation between elevation, latitude and longitude (Table 1) which was negatively correlated with longitude and latitude, while positively with elevation. In February, the highest (73-100 mm) was recorded in Guilan Province (though revealing a reduction compared to January), while the lowest (34-41 mm) in the west of Golestan Province (Fig. 5).

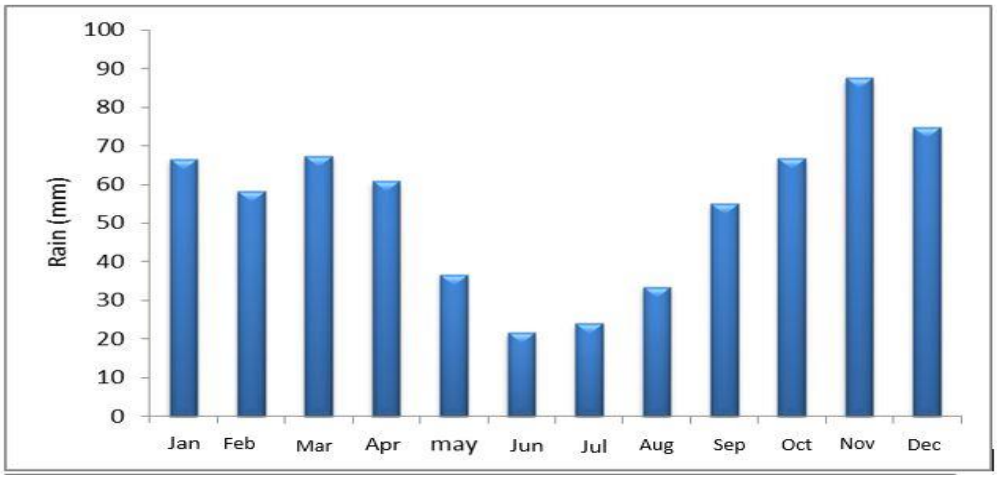

Fig. 2. Average monthly precipitation for the SCS.

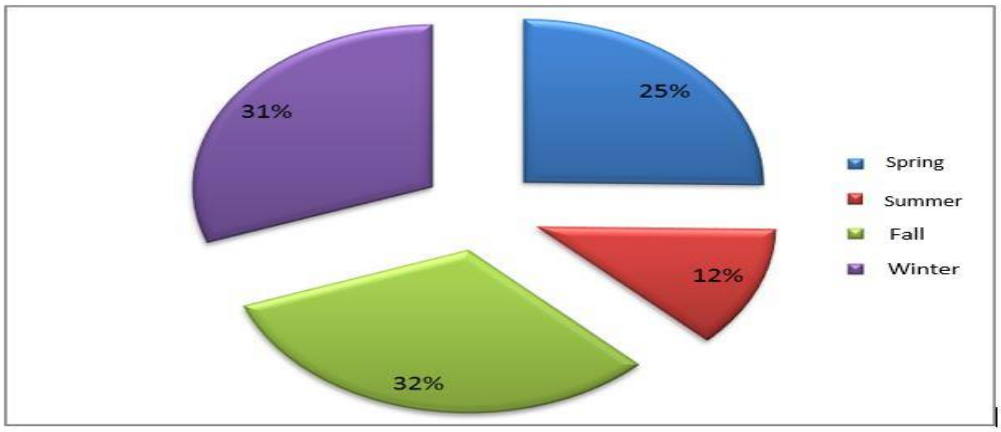

Fig. 3. Seasonal distribution of precipitation for the SCS.

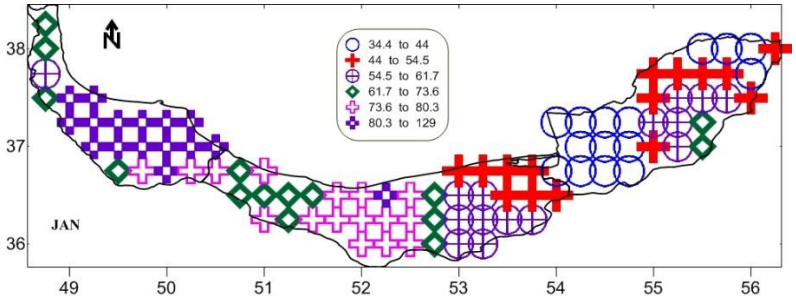

Fig. 4. Average precipitation (0.25° resolution) derived from TRMM 3B43 in January during the period of 1998-2013.

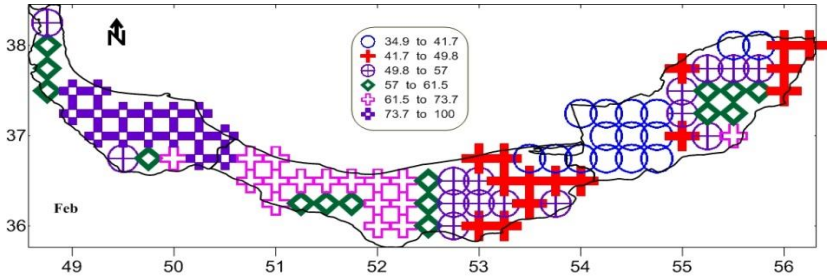

Fig. 5. Average precipitation (0.25° resolution) derived from TRMM 3B43 in February during the study period of 1998-2013.

Similar to the previous two months, the highest precipitation (84-102 mm) in March was recorded in Guilan Province and the west of the Caspian Sea, while the lowest (39-49 mm) in the western parts of Golestan Province (Fig. 6). In April, the maximum precipitation (79-98 mm) was recorded in two separate regions in the south and west of Guilan Province (west and south of the Caspian Sea), while the lowest (32-37 mm) in the northwest of Golestan and eastern parts of Caspian Sea exhibiting a change of precipitation patterns compared to previous months (Fig. 7).

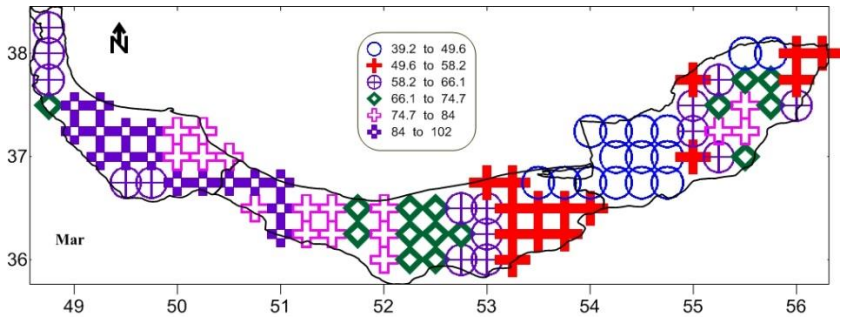

Fig. 6. Average precipitation (0.25° resolution) derived from TRMM 3B43 in March during the study period of 1998-2013.

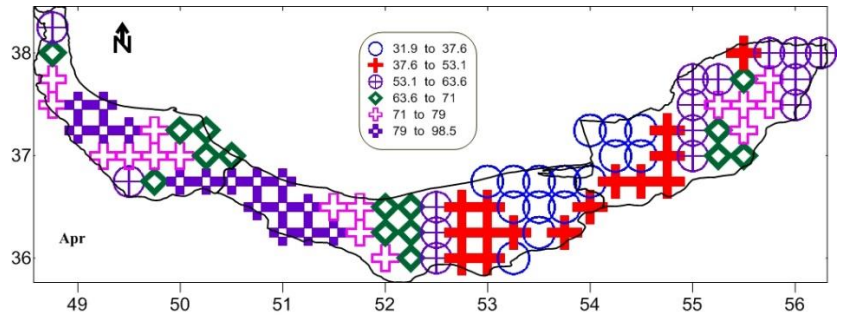

Fig. 7. Average precipitation (0.25° resolution) derived from TRMM 3B43 in April during the study period of 1998-2013.

In May, the highest precipitation (48-60 mm) was recorded in Guilan Province and the west of the Caspian Sea, while the lowest in January in the west of Golestan Province and eastern parts of the sea (34-44 mm; Fig. 8). The precipitation was analyzed using the Pearson correlation between elevation, latitude and longitude (Table 1). It was negatively correlated with longitude, while positively with elevation and latitude. In June, the highest precipitation (30-41 mm) was recorded in Guilan Province, while the lowest (10-15 mm) in the western and eastern parts of Golestan Province (Fig. 9). It was also inversely correlated with longitude and latitude, while positively with elevation (Table 1).

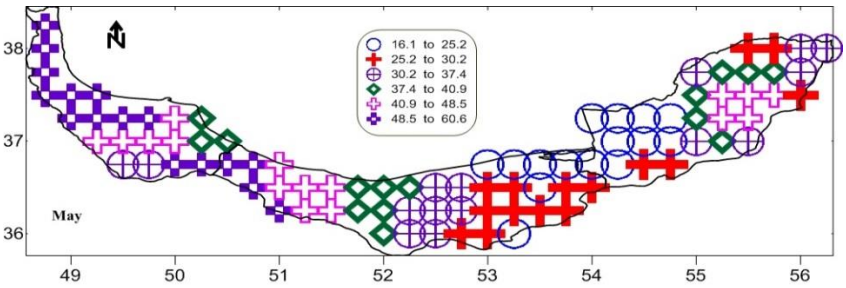

Fig. 8. Average precipitation (0.25° resolution) derived from TRMM 3B43 in May during the study period of 1998-2013.

In July, the highest precipitation (29-49 mm) was recorded in Guilan Province, while the lowest (10-15 mm) in the west and northeast of Golestan Province (Fig. 10). The precipitation was analyzed using the Pearson correlation between elevation, latitude and longitude (Table 1). It was inversely correlated with longitude elevation and latitude. In August, the highest precipitation (40-81 mm) was recorded in Guilan Province, while

the lowest (15-18 mm) in the west and northeast of Golestan Province (Fig. 11).It was negatively correlated with longitude and elevation, while positively with latitude (Table 1).

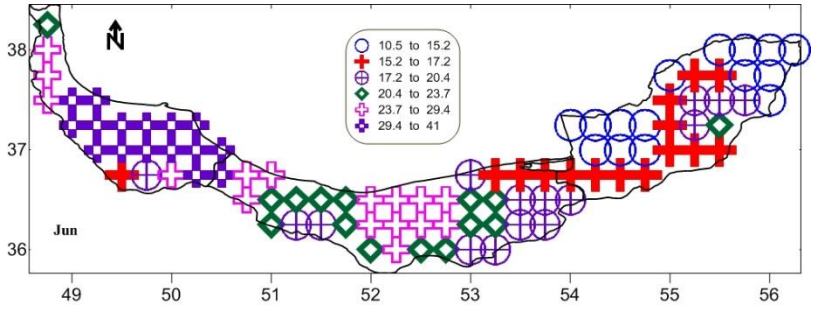

Fig. 9. Average precipitation (0.25° resolution) derived from TRMM 3B43 in June durin the study period of 1998-2013.

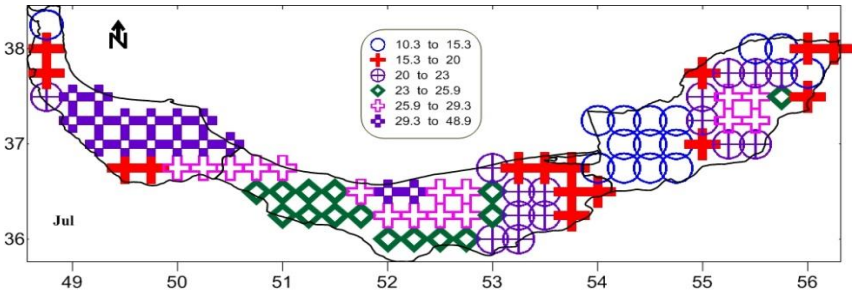

Fig. 10. Average precipitation (0.25° resolution) derived from TRMM 3B43 in July during the study period of 1998-2013.

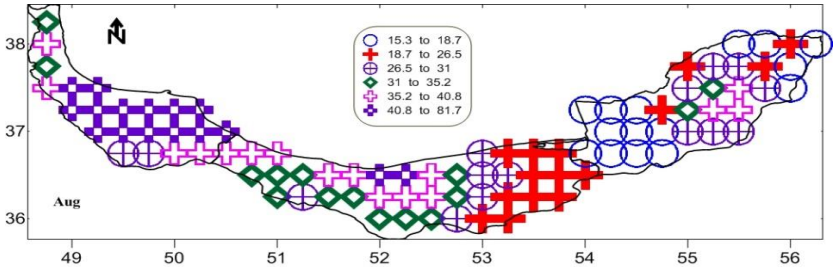

Fig. 11. Average precipitation (0.25° resolution) derived from TRMM 3B43 in August during the study period of 1998-2013.

In September, the highest precipitation (84-152 mm) was recorded in Guilan Province, while the lowest (16-26 mm) in the northwest and northeast of Golestan Province (Fig. 12). The precipitation analysis was conducted using Pearson correlation between elevation, latitude and longitude (Table 1). It was negatively correlated with longitude, latitude and elevation. In October, the highest precipitation (108-152 mm) was recorded in Guilan Province, while The lowest (19-28 mm) in the northwest and northeast of Golestan Province (Fig. 13). It was inversely correlated with longitude and latitude, while positively with elevation (Table 1).

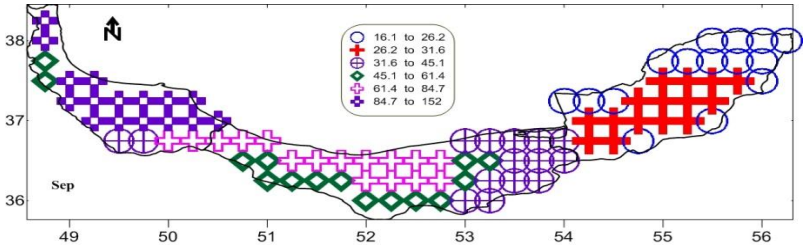

Fig. 12. Average precipitation (0.25° resolution) derived from TRMM 3B43 in Sepember during the study period of 1998-2013.

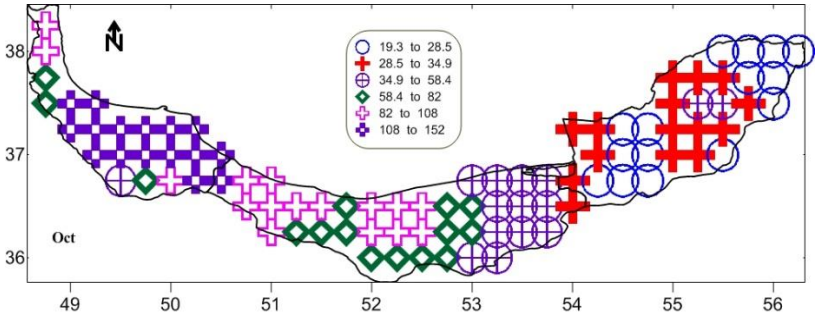

Fig. 13. Average Precipitation (0.25° resolution) derived from TRMM 3B43 in October during the study period of 1998-2013.

In November, the highest precipitation (134-201 mm) was recorded in Guilan Province, while the lowest (32-44 mm) in the west and northeast of Golestan Province (Fig. 14). The precipitation was analyzed based on the Pearson correlation between elevation, latitude and longitude (Table 1). It was negatively correlated with longitude and latitude, while positively with elevation. The highest inverse correlation (0.87) at a significant level of 0.01 was observed between rain and longitude in this month. In December, the highest precipitation (110-168 mm) was recorded in Guilan Province, while the lowest (26-35 mm) in the west and northeast of Golestan Province (Fig. 15). It was negatively correlated with longitude and latitude, while positively with elevation (Table 1).

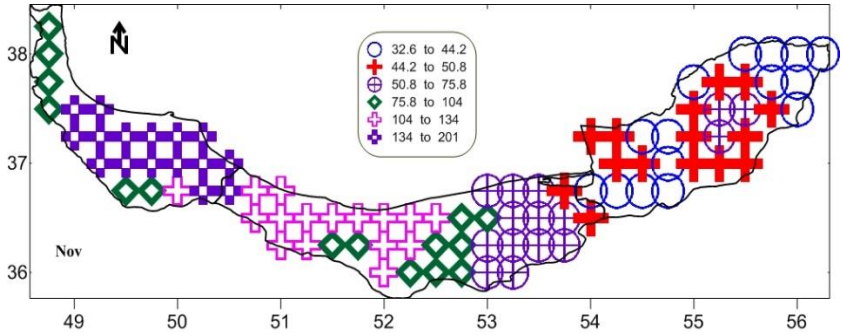

Fig. 14. Average precipitation (0.25° resolution) derived from TRMM 3B43 in November during the study period of 1998-2013.

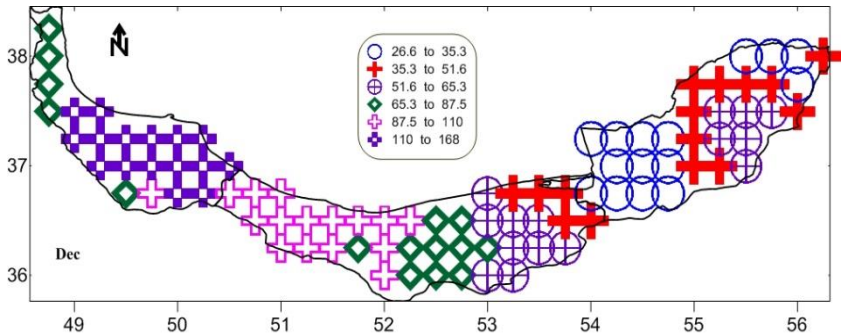

Fig. 15. Average precipitation (0.25° resolution) derived from TRMM 3B43 in October during the study period of 1998-2013.

In spring, the highest precipitation (70-79 mm) was recorded at the center of Guilan Province and the west of the Caspian Sea, while the lowest (29-38 mm) in the western areas of Golestan Province and east of Caspian Sea (Fig. 16). It was analyzed using the Pearson correlation between elevation, latitude and longitude (Table 1). It was inversely correlated with longitude, while positively with elevation and latitude. In summer, the highest precipitation (32-56 mm) was recorded in Guilan Province and the center of Caspian Sea, while the lowest (12-15 mm) in the western and eastern areas of Golestan Province (Fig. 17). It was negatively related to longitude, latitude and elevation (Table 1).

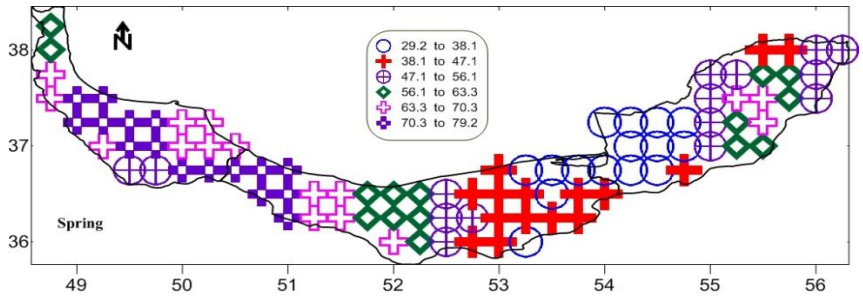

Fig. 16. Average Precipitation (0.25° resolution) derived from TRMM 3B43 in spring during the study period of 1998-2013.

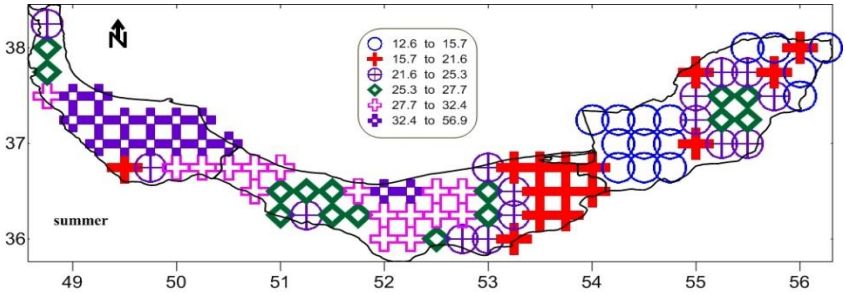

Fig. 17. Average precipitation (0.25° resolution) derived from TRMM 3B43 in summer during the study period of 1998-2013.

In autumn, the highest precipitation (107-168 mm) was recorded in Guilan Province, while the lowest (22-32 mm) in the west and northeast of Golestan Province (Fig. 18). The precipitation analysis was conducted using Pearson correlation between elevation, latitude and longitude (Table 1). It was negatively related to longitude and latitude, while positively related to elevation. The highest inverse correlation (0.862) at a significant level of 0.01 was observed between rain and longitude in this season. In winter, the highest precipitation (87-132 mm) was recorded in Guilan Province, while the lowest (33-41 mm) in the western and eastern areas of Golestan Province (Fig. 19). It was negatively correlated with longitude and latitude, while positively with elevation (Table 1).

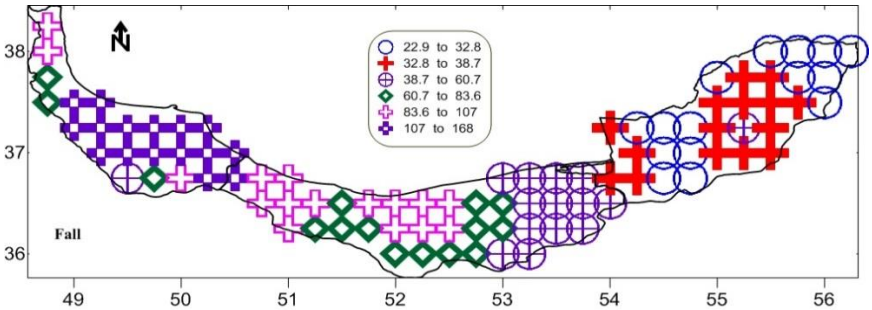

Fig. 18. Average precipitation (0.25° resolution) derived from TRMM 3B43 in autumn during the study period of 1998-2013.

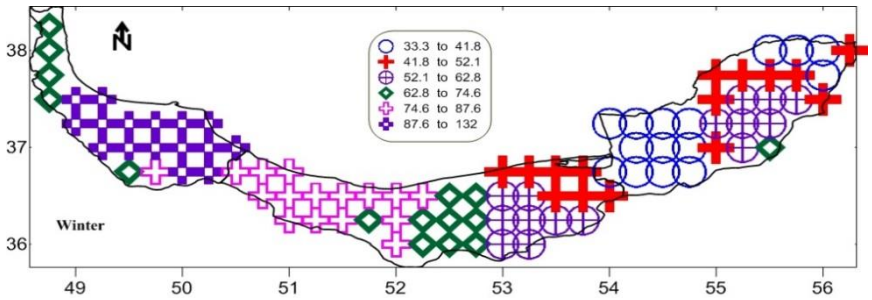

Fig. 19. Average precipitation (0.25° resolution) derived from TRMM 3B43 in winter during the study period of 1998-2013.

The highest annual precipitation (892-1305 mm) was observed in Guilan Province. The precipitation declined toward the east of Golestan Province. In addition, the lowest annual precipitation (321-393 mm) was recorded in the west and northeast of Golestan Province. According to Fig. 20, the precipitation patterns are relatively longitudinal. The precipitation data was analyzed using as Pearson correlation between elevation, latitude and longitude (Table 1). It was positively correlated with elevation and there was a strong inverse relationship between rain and longitude.

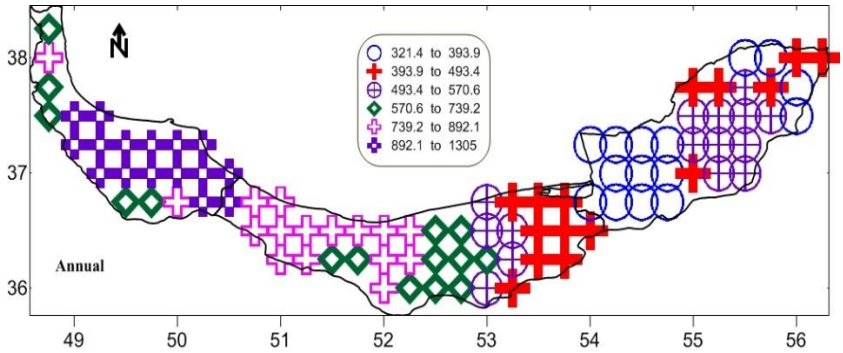

Fig. 20. Average annual rain (0.25° resolution) derived from TRMM 3B43 during the study period of 1998-2013.

CONCLUSION

In this study, the spatial and temporal precipitation patterns were studied for 92 cells in the south of the Caspian Sea based on monthly, seasonal and annual time scales using data derived from TRMM 3B42 over a period of 16 years (1998-2013). Also, to account for the impact of geographical conditions such as elevation, latitude and longitude on precipitation, the Pearson correlation was adopted. There was a strong inverse correlation between rain and longitude, and the highest correlation was observed in the autumn, especially in November. However, it was not correlated with elevation and latitude at a significance level of 0.01. The highest average annual precipitation was recorded in Guilan Province. Since precipitation had a tendency to decline towards the east of Golestan Province, the lowest annual precipitation was recorded in the west and northeast of Golestan Province. Except for April, March and May, the highest precipitation pattern was observed during the spring in Guilan Province. In the months preceding this period, the west of the Caspian Sea had the second highest precipitation pattern in the study area. Meanwhile, the precipitation pattern in spring, such as the rest of abovementioned months, was inconsistent with other seasons. The lowest precipitation patterns were registered in the western and eastern regions of Golestan Province, However, in April and May, the lowest precipitation patterns were observed in the western regions of Golestan and the east of the Caspian Sea.

REFERENCES

Ahmadi, M & Narangifard, M 2012, Assessment precipitation regions in Fars Province using TRMM satellite data. *Researches in Earth Sciences*, 3(11): 28-44.

Akbari Yangehghaleh, M, sanaeinejad, S, Faridhosseini, A & Akbari, M 2018, The study of spatial -temporal distribution of rain, using TRMM data (Case study: Khorasan Razavi Province). *Journal of Climate Research*, 7: 1-18.

Almazroui, M 2011, Calibration of TRMM rainfall climatology over Saudi Arabia during 1998-2009. *Atmospheric Research*, 99: 400-414.

Chen, C, Yu, Z, Li, L, & Yang, C 2011, Adaptability evaluation of TRMM satellite rainfall and its application in the Dongjiang River Basin". *Procedia Environmental Sciences*, 10: 396-402. DOI: 10.1016/j.proenv. 2011.09.065.

Du, L, Tian, Q, Yu, T, Meng, Q, Jancso, T, Udvardy, P & Huang, Y 2013, A comprehensive drought monitoring method integrating MODIS and TRMM data. *International Journal of Applied Earth Observation and Geoinformation*, 23: 245-253. doi.org/10.1016/j.jag.2012.09.010.

Duncan, JM, & Biggs, EM 2012, Assessing the accuracy and applied use of satellite-derived precipitation estimates over Nepal. *Applied Geography*, 34: 626-638. DOI:10.1016/j.apgeog.2012.04.001

Gabella, M, Morin, E, Notarpietro, R & Michaelides, S 2013, Winter precipitation fields in the Southeastern Mediterranean area as seen by the Ku-band Space borne weather radar and two C-band ground-based radars. *Atmospheric Research*, 119: 120-130.

Huffman, GJ, Bolvin, DT, Nelkin, EJ, Wolff, DB, Adler, RF, Gu, G, Hong, Y, Bowman, KP & Stocker, EF 2007, The TRMM multisatellite precipitation analysis (TMPA): quasi-global, multiyear, combined-sensor precipitation estimates at fine scales. *Journal of Hydrometeorol*ogy, 8: 38-55.

Immerzeel, WW, Rutten, MM, & Droogers, P 2009, Spatial downscaling of TRMM precipitation using vegetative response on the Iberian Peninsula. *Remote Sensing of Environment*, 113: 362-370. DOI:10.1016/j.rse.2008.10.004.

Javanmard, S & Jamli, B J 2015, The study of atmospheric physics parameters over Iran using satellite TRMM-TMI data. *Journal of Earth Science & Climatic Change*, 6:17. DOI: 10.4172/2157-7617.1000281

Javanmard, S, Yatagai, A, Nodzu, M I, BodaghJamali, J & Kawamoto, H 2010, Comparing high-resolution gridded precipitation data with satellite rainfall estimates of TRMM_3B42 over Iran. *Advances in Geosciences*, 25: 119-125. DOI: 10.5194/adgeo-25-119-2010.

Jia, S, Zhu, W, Lű, A, & Yan, T 2011, A statistical spatial downscaling algorithm of TRMM precipitation based on NDVI and DEM in the Qaidam Basin of China. *Remote sensing of Environment*, 115: 3069-3079.

Kaufman, L & Rousseeuw, PJ 2009, Finding groups in data: An introduction to cluster analysis. 344. John Wiley & Sons.

Kummerow, C, Barnes, W, Kozu, T, Shiue, J, Simpson, J 1998, The Tropical rainfall Measuring Mission (TRMM) sensor package. *Journal of Atmospheric and Oceanic Technology*, 15: 809-817.

Kummerow, C 2000, The status of the Tropical rainfall Measuring Mission (TRMM) after two years in orbit. *Journal of Applied Meteorology*, 39: 1965-1982.

Li, X H, Zhang, Q, & Xu, C Y 2012, Suitability of the TRMM satellite Precipitation s in driving a distributed hydrological model for water balance computations in Xinjiang catchment, Poyang Lake basin. *Journal of Hydrology*, 426: 28-38.

Liu, Q, & Fu, Y 2010, Comparison of radiative signals between precipitating and non-precipitating clouds in frontal and typhoon domains over East Asia. *Atmospheric Research*, 96: 436-446.

Mishra, A K, Gairola, R M, & Agarwal, V K 2012, Rainfall estimation from combined observations using KALPANA-IR and TRMM-precipitation radar measurements over Indian region. *Journal of the Indian Society of Remote Sensing*, 40: 65-74.

Moazami, S, Golian, S, Kavianpour, M R, & Hong, Y 2013, Comparison of PERSIANN and V7 TRMM Multi-satellite Precipitation Analysis (TMPA) products with rain gauge data over Iran. *International Journal of Remote Sensing*, 34: 8156-8171. doi.org/10.1080/01431161.2013.833360.

Moffitt, C B, Hossain, F, Adler, R F, Yilmaz, K K, & Pierce, H F 2011, Validation of a TRMM-based global flood detection system in Bangladesh. *International Journal of Applied Earth Observation and Geoinformation*, 13:165-177.

Mozafari, G A, & Narangifard, M 2015, The vegetative cover deterioration due to the droughts on the Mulla Sadra watershed and application of remote sensing techniques in its monitoring. *Water Engineering*, 8: 1-14.

Okamoto, K, Miyazaki, S, & Ishida, T 1979, Remote sensing of precipitation by a satellite-borne microwave remote sensor. *Acta Astronautica*, 6: 1043-1060.

Omidvar, K & Narangifard, M 2015, Study of distribution temporal– spatial the probable maximum precipitation (PMP) in Fars Province. *Applied Climatology*, 2: 17-36.

Puri, S, Stephen, H, & Ahmad, S 2011, Relating TRMM precipitation radar land surface backscatter response to soil moisture in the southern United States. *Journal of Hydrology*, 402: 115-125.

Puri, S, Stephen, H, & Ahmad, S 2011, Relating TRMM precipitation radar backscatter to water stage in wetlands. *Journal of Hydrology*, 401: 240-249.

Roohi, A, Yasin, Z, Kideys, A E, Hwai, A T S, Khanari, A G & Eker-Develi, E 2008, Impact of a new invasive ctenophore (*Mnemiopsis leidyi*) on the zooplankton community of the Southern Caspian Sea. *Marine Ecology*, 29: 421-434.

Shirvani, A & Fakhari Zade Shirazi, E 2014, Comparison of ground based observation of precipitation with TRMM satellite estimations in Fars Province. *Journal of Agricultural Meteorology*, 2:1-15.

Shrivastava, R, Dash, SK, Hegde, MN, Pradeepkumar, KS & Sharma, DN 2014, Validation of the TRMM multi satellite rainfall product 3B42 and estimation of scavenging coefficients for 131I and 137Cs using TRMM 3B42 rainfall data. *Journal of Environmental Radioactivity*, 138: 132-136.

Siabi, N, Sanaeinejad, S & Ghahraman, B 2017, Evaluation of rainfall data derived from TRMM satellite, MM5 model and ground observation using sapatio-temporal analysis in arid and semi-arid mountainous area. *Geography and Environmental Hazards*, 6: 163-179.

Sotodeh, F & Alijani, B 2015, The relationship between spatial distribution of heavy precipitation and pressure patterns in guilan province. *Journal of Spatial Analysis Environmental Hazarts*, 2: 63-73.

Ud din, S, Al-Dousari, A, Ramdan, A & Al Ghadban, A 2008, Site-specific precipitation estimate from TRMM data using bilinear weighted interpolation technique: An example from Kuwait. *Journal of Arid Environments*, 72: 1320-1328.

Varikoden, H, Samah, AA & Babu, CA 2010, Spatial and temporal characteristics of rain intensity in the Peninsular Malaysia using TRMM rain rate. Journal of hydrology, 387: 312-319.

Bibliographic information of this paper for citing:

Omidvar, K, Narangifard, M, Fatemi, M 2022, Analyzing the relationship between geographical elements and precipitation patterns in the southern shores of the *Caspian Sea*. Caspian Journal of Environmental Sciences, 20: 89-99.